

Recent Timing Studies on RXTE Observations of 4U 1538-52

A. Baykal¹, S.Ç. İnam² and E. Beklen^{1,3}

¹ Physics Department,

Middle East Technical University, 06531 Ankara, Turkey

altan@astroa.physics.metu.edu.tr

² Department of Electrical and Electronics Engineering,

Başkent University, 06530 Ankara, Turkey

inam@baskent.edu.tr

³ Physics Department,

Süleyman Demirel University, 32260, Isparta, Turkey

elif@astroa.physics.metu.edu.tr

Abstract. The high mass X-ray binary pulsar 4U 1538-52 was observed between July 31 and August 7, 2003. Using these observations, we determined new orbital epochs for both circular and elliptical orbit models. The orbital epochs for both orbit solutions agreed with each other and yielded an orbital period derivative $\dot{P}/P = (0.4 \pm 1.8) \times 10^{-6} \text{ yr}^{-1}$. This value is consistent with the earlier measurement of $\dot{P}/P = (2.9 \pm 2.1) \times 10^{-6} \text{ yr}^{-1}$ at the 1σ level and gives only an upper limit to the orbital period decay. Our determination of the pulse frequency showed that the source spun up at an average rate of $2.76 \times 10^{-14} \text{ Hz sec}^{-1}$ between 1991 and 2003.

Key words. X-rays:binaries; Stars:neutron; pulsars:individual:4U 1538-52; accretion, accretion disks

1. Introduction

The source 4U 1538-52 was discovered using the Uhuru satellite (Giacconi et al. 1974). X-ray pulsations with a period of 529 seconds were detected from two independent satellite experiments: Ariel 5 (Davidson 1977) and OSO-8 (Becker et al., 1977). OSO-8 observations also revealed a clear orbital modulation at 3.7 days and evidence of an eclipse lasting ~ 0.51 days. The optical companion of 4U 1538-52 was identified to be the B0 I giant QV

Nor (Parkes, Murdin & Mason 1978). BATSE observations of this source permitted the construction of long-term pulse frequency and intensity histories (Rubin, Finger, Scott et al. 1997). In the pulse frequency history, Rubin et al. (1997) found short-term pulse frequency changes of either sign, and a power density spectrum of fluctuations of the pulse frequency derivative that is consistent with white torque noise on timescales from 16 to 1600 days.

From RXTE observations, Clark (2000) obtained new orbital parameters of the source which provided marginal evidence of orbital decay, i.e., they found $\dot{P}_{orb}/P_{orb} = (-2.9 \pm 2.1) \times 10^{-5} \text{ yr}^{-1}$. In this work, we present new orbital epoch and pulse frequency measurements based on our analysis of archival RXTE observations of 4U 1538-52.

2. Observations

The observations of 4U 1538-52 took place between July 31 and August 7, 2003 (MJD 52851 - 52858) and accumulated a total nominal exposure of ~ 75 ksec. The results presented here are based on data collected with the Proportional Counter Array (PCA, Jahoda et al., 1996). The PCA instrument consists of an array of five collimated xenon/methane multianode proportional counters. The total effective area is approximately 6250 cm^2 and the field of view is $\sim 1^{\circ}$ FWHM. The nominal energy range of the PCA extends from 2 to 60 keV.

3. Determination of Orbital Epoch and Pulse Frequency

Background light curves and X-ray spectra were generated by using background estimator models based on the rate of very large events (VLE), detector activation, and cosmic X-ray **background**. The background light curves were subtracted from the source light curve obtained from the binned Good Xenon data. **For 4U 1538-52, X-ray emission coming from the galactic ridge is only a few percent of the total X-ray emission which should not affect our timing analysis (see Makishima et al. 1987), so we did not include an estimation of the galactic ridge emission in our analysis.** In Figure 1, we present the background subtracted light curve. Although the number of active PCUs varied from 1 to 4 during the observations, Figure 1 shows count rates adjusted as if 5 PCUs had been active using the "correctle" tool in HEASOFT 6. For the timing analysis, we corrected the light curve to the barycenter of the solar system. We also corrected this barycentered light curve for binary orbital motion using both circular and elliptical orbital models given in Table 1 (see also Clark (2000)). Then a template pulse profile was created by folding the light curve into one master profile. Pulse profiles were also made from each of the 12 independent RXTE observations seen in Figure 1.

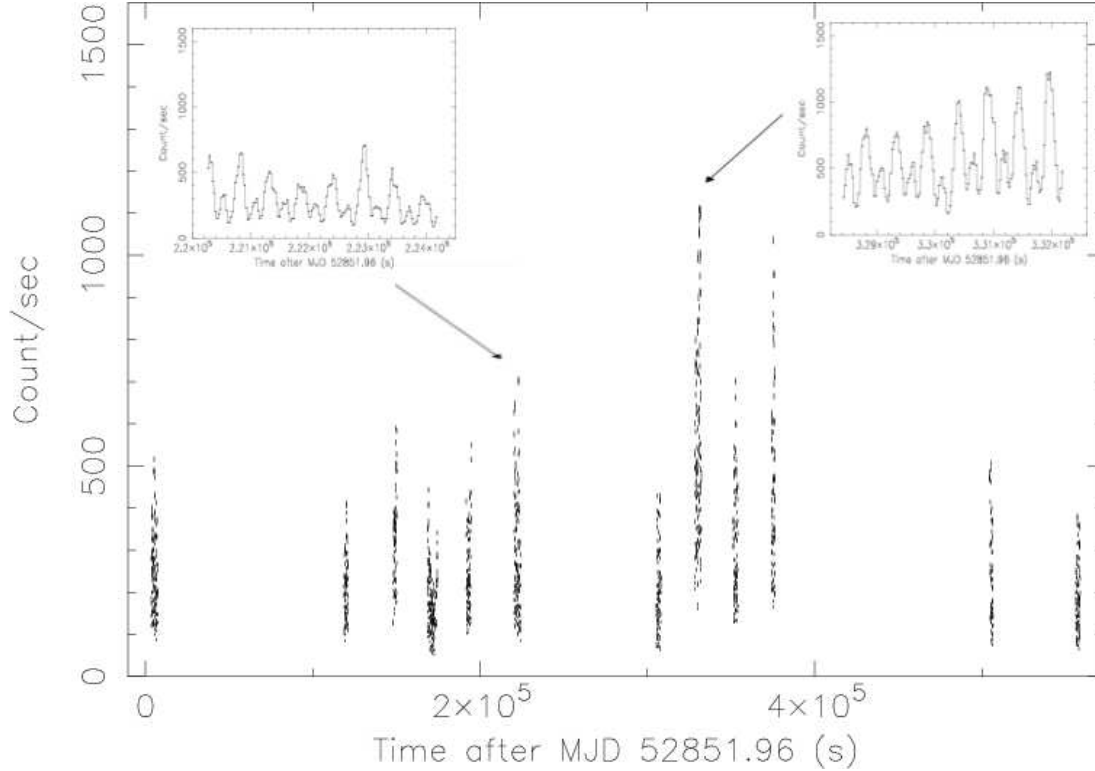


Fig. 1 – 2-30 keV RXTE-PCA light curve of 4U 1538-52 between July 31 and August 7, 2003. Two 26s binned \sim 3ksec samples of this light curve corresponding to single RXTE orbits are presented on the upper left and the upper right.

In order to find the pulse frequency and a new orbital epoch, we obtained 12 pulse arrival times through the \sim 2 binary orbits using **a cross-correlation technique**. In the pulse timing analysis, we used the method of harmonic representation of pulse profiles, which was proposed by Deeter & Boynton (1985). In this method, the pulse profiles for each orbit and the master profile are expressed in terms of harmonic series. We used 10-term unweighted harmonic series to cross-correlate the template pulse profile with the pulse profiles for each RXTE observation. The maximum value of the cross-correlation is analytically well-defined and does not depend on the phase binning of the pulses.

The source 4U 1538-52 has a variable pulse profile which affects the pulse timing. In order to estimate the errors in the arrival times, the light curve of each RXTE observation was divided into approximately 4-5 equal subsets and new arrival times were estimated. The standard deviation of the arrival **times** obtained from each subset of the observation was taken to be the uncertainty in the arrival time for that observation.

Arrival time delays may arise from the change of the pulse frequency during the observation (or intrinsic pulse frequency derivative) and from the **differences between the assumed and actual orbital and pulse parameters** (Deeter, Boynton and Pravdo 1981),

$$\delta\phi = \phi_o + \delta\nu(t - t_o) + \frac{1}{2}\dot{\nu}(t - t_o)^2 - \delta\nu\frac{2\pi\delta T_{\pi/2}}{P_{orbit}}\frac{asini}{c}\cos l_n \quad (1)$$

where $\delta\phi$ is the pulse phase offset deduced from the pulse timing analysis, t_o is the mid-time of the observation, ϕ_o is the residual phase offset at t_o , ν is the pulse frequency at time t_o , $\dot{\nu}$ is the pulse frequency derivative of the source, $T_{\pi/2}$ is the orbital epoch when the mean orbital longitude is equal to 90 degrees, P_{orbit} is the orbital period and $l_n = 2\pi(t_n - T_{\pi/2})/P_{orbit} + \pi/2$ is the mean orbital longitude at t_n . Corrected values of orbital **and pulse** parameters $\delta\nu$, $\delta T_{\pi/2}$ and $\dot{\nu}$ were estimated from the fits of above expression to pulse phase residuals.

Table 1 presents the result of fits for both orbital and pulse parameters.

We also reestimated the orbital epochs by varying the projected orbital radius $(a_x/c)\sin i$ in the range of its uncertainty ($\pm 1\sigma$) and found that the resulting orbital epochs are consistent with the best fit value at the 1σ level. The error in the orbital epoch due to an error in $(a_x/c)\sin i$ may also be expressed (Deeter, Boynton and Pravdo 1981) as

$$\sigma_{T_{\pi/2}} = \frac{P_{orb}\sigma_{(a_x/c)\sin i}}{2\pi a_x/c\sin i} \sim 0.0073\text{days} \quad (2)$$

where $\sigma_{a_x/c\sin i}$ is the uncertainty in the projected orbital radius. This value is small relative to our error estimate for the orbital epoch (see Table 1). In Figure 2, we present the arrival time delay, the best fit elliptical orbit model, and arrival time residuals.

As seen from Table 1, the orbital epochs for circular and elliptical orbital models agree with each other at the 1σ level. In order to check our technique, we extracted observations of 4U 1538-52 done in 1997 (MJD 50449.93-50453.69) and estimated orbital epochs for those observations. The results agreed with the orbital epochs given by Clark (2000).

In Table 2, we present the orbital epoch measurements from different observatories and orbital cycle number (n). In Figure 3, we present observed minus calculated values of orbital epochs ($T_{\pi/2} - n \langle P_{orbit} \rangle - \langle T_{\pi/2} - n \langle P_{orbit} \rangle \rangle$) relative to the constant orbital period ($\langle P_{orbit} \rangle = 3.7228366$ days). A quadratic fit to the epochs from all experiments yielded an estimate of the rate of period change $\dot{P}_{orb}/P_{orb} = (0.4 \pm 1.8) \times 10^{-6} \text{yr}^{-1}$. In Figure 4, we display the long-term pulse frequency history of the source.

4. Discussion

Before CGRO observations, 4U 1538-52 had been found to have a long-term spin down trend. A linear fit to pre-CGRO pulse frequency history gives $\dot{\nu}/\nu \sim -8 \times 10^{-12} \text{s}^{-1}$ and a linear fit to CGRO and our RXTE result yields $\dot{\nu}/\nu \sim 1.45 \times 10^{-11} \text{s}^{-1}$. Rubin et al (1997) constructed the power spectrum of pulse frequency derivative fluctuations. Their analysis showed that the pulse frequency derivative fluctuations can be explained on timescales from 16 to 1600 days with an average white noise strength of $(7.6 \pm 1.6) \times 10^{-21} (\text{Hz s}^{-1})^2 \text{Hz}^{-1}$. A random walk in pulse frequency (or white noise in pulse frequency derivative) can be explained as a sequence of **steps in pulse frequency with an RMS value of $\langle (\delta\nu^2) \rangle$** which occur at a constant rate R . Then the RMS variation

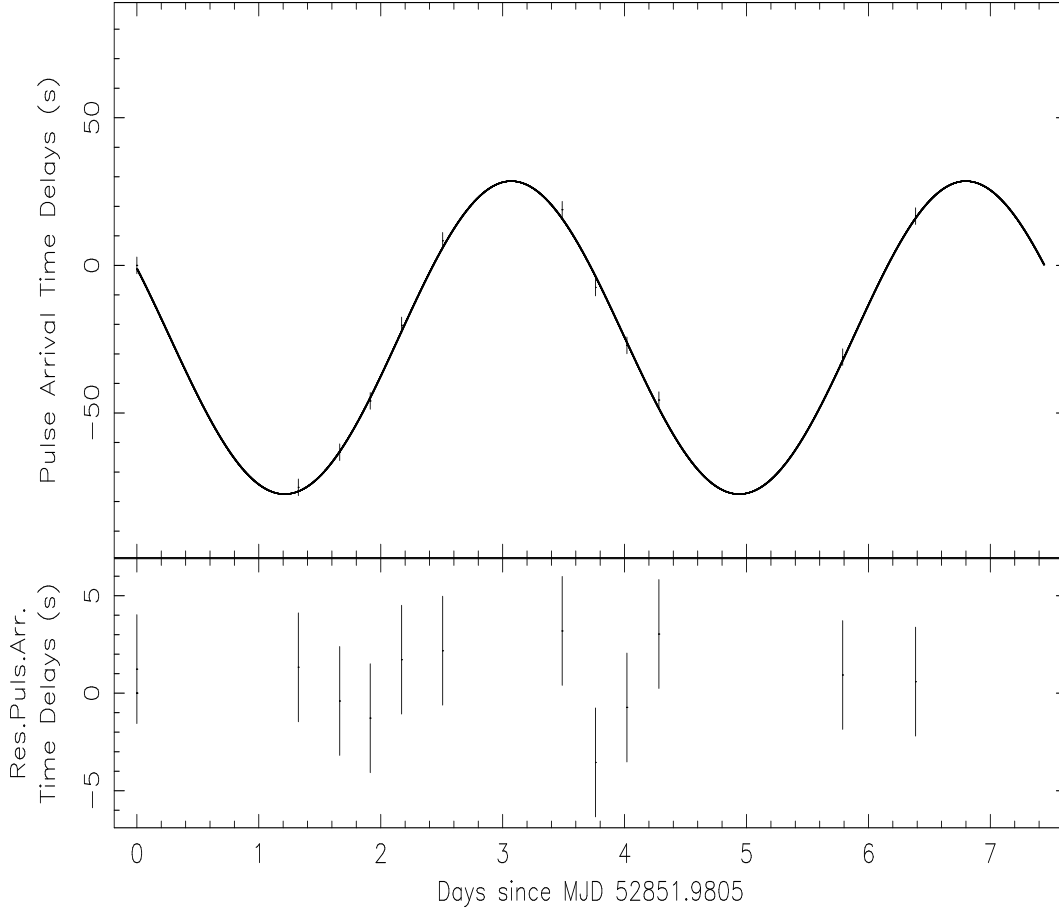


Fig. 2 – **(Top)** Pulse arrival time delays and best-fit elliptical orbital model given in Table 1.

(Note that pulse profiles are obtained with respect to the reference time 52855.0585 MJD).

(Below) Residuals after removing best orbital model.

of the pulse frequency scales with elapsed time τ as $\langle (\Delta\nu)^2 \rangle = R \langle (\delta\nu)^2 \rangle \tau$ (Hz), where $S = R \langle \delta\nu^2 \rangle$ is defined as noise strength. Then, RMS scaling for the pulse

Table 1. Orbital Parameters of 4U 1538-52

Parameter	Elliptical Orbit	Circular Orbit
$T_{\pi/2}$ Orbital Epoch (MJD)	52855.0421 ± 0.025	52855.0441 ± 0.025
$a_x \sin i$ (lt-s) ^a	56.6 ± 0.7	54.3 ± 0.6
e^a	0.174 ± 0.015	
ω^a (deg)	64 ± 9	
P_{orbit}^a	3.7228366 ± 0.000032	3.7228366 ± 0.000032
Epoch (MJD)	52855.0585 ± 0.025	52855.0585 ± 0.025
P_{pulse} (s)	526.8551 ± 0.016	526.8535 ± 0.013
$\dot{\nu}$ (Hz s ⁻¹)	$(2.838 \pm 4.124) \times 10^{-13}$	$(2.241 \pm 2.764) \times 10^{-13}$
reduced χ^2	1.44	1.0

^a Taken from Clark (2000)

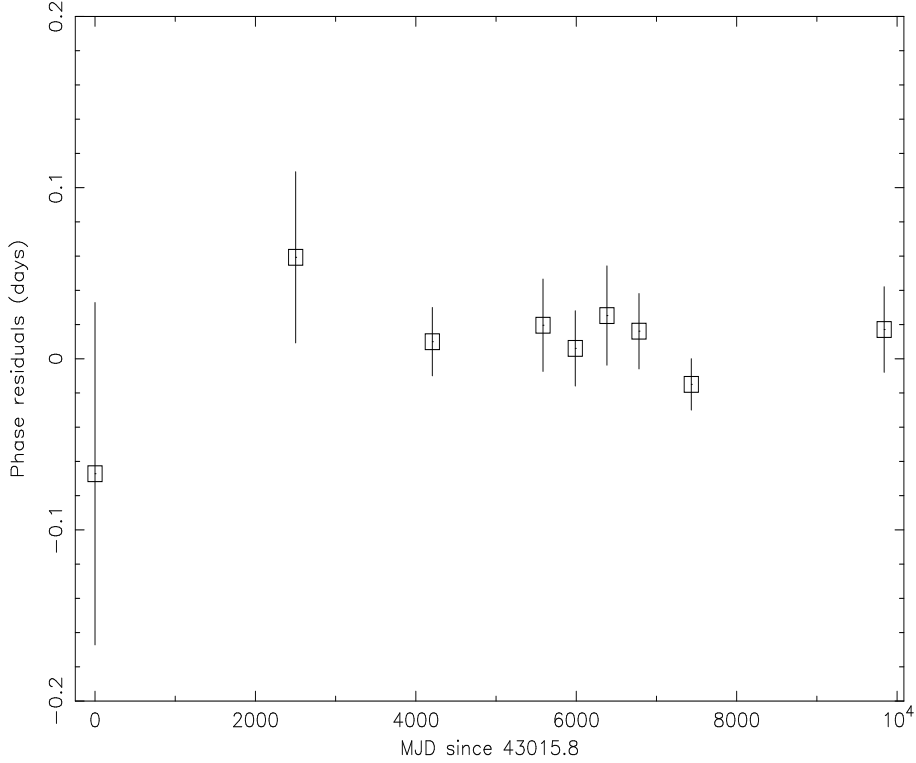


Fig. 3 – The phase residuals of orbital epoch for 4U 1538-52. The orbital phases are estimated relative the constant orbital period ($T_{\pi/2} - n \langle P_{orbit} \rangle - \langle T_{\pi/2} - n \langle P_{orbit} \rangle \rangle$), where n is the orbital cycle number (see Table 2). The rightmost point corresponds to the most recent RXTE observation of ID 80016.

frequency derivatives can be obtained as $\langle (\Delta\dot{\nu})^2 \rangle^{1/2} = (S/\tau)^{1/2} \text{Hz.s}^{-1}$. As seen from Table 1, in our fits, upper limits on intrinsic pulse frequency derivatives are 7-10 times higher than the long-term spin up rates. If white noise in the pulse frequency derivative can be interpolated to a few days, **then the upper limit on the change of** frequency derivative obtained from a ~ 1 week observation should typically have a magnitude

Table 2. Orbital epochs by pulse timing analysis

Experiment	Orbit Number	Orbital Epoch (MJD)	Reference
OSO 8	-1128	43015.800 ± 0.1	Becker et al., 1977
Tenma	-457	45517.660 ± 0.050	Makishima et al., 1987
Ginga	0	47221.474 ± 0.020	Corbet et al., 1993
BATSE	370	48600.979 ± 0.027	Rubin et al., 1997
BATSE	478	49003.629 ± 0.022	Rubin et al., 1997
BATSE	584	49398.855 ± 0.029	Rubin et al., 1997
BATSE	691	49797.781 ± 0.022	Rubin et al., 1997
RXTE	866	50450.206 ± 0.014	Clark 2000
RXTE	1511	52855.0421 ± 0.025	present work

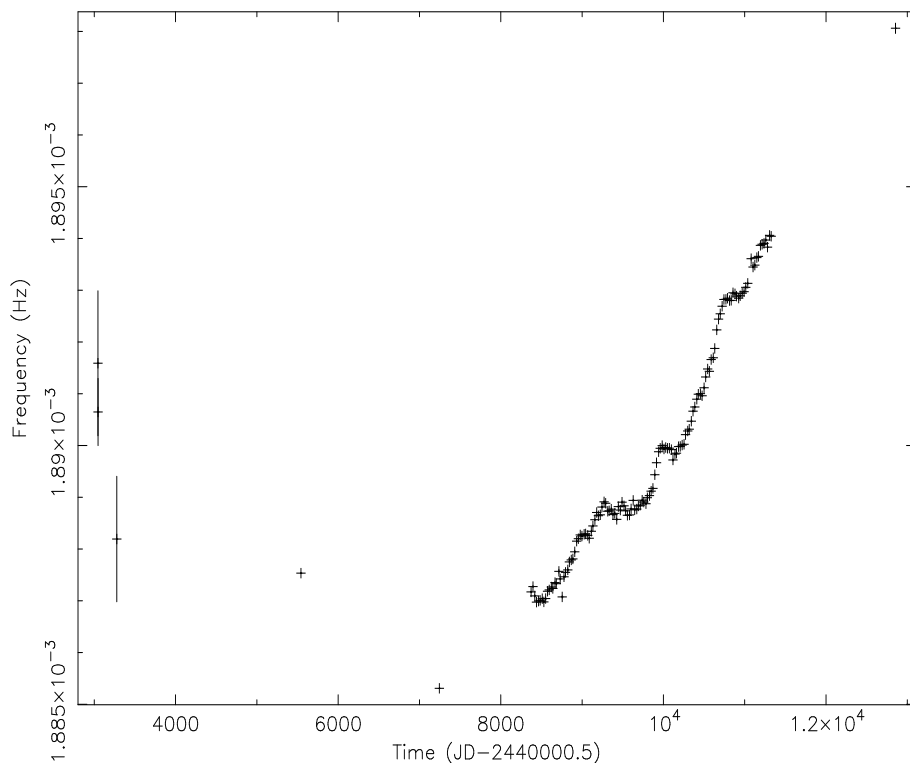


Fig. 4 – Pulse frequency history of 4U 1538-52. The rightmost point corresponds to most recent RXTE observation of ID 80016.

that can be estimated from $\langle (\Delta\dot{\nu})_{week}^2 \rangle = \langle (\Delta\dot{\nu})_{1600days}^2 \rangle \times 15^2$ **This value is 15/7 - 15/10 times higher than the measured upper limit values. Therefore the measured upper limits on the intrinsic pulse frequency derivatives for 1 week are consistent with the values from the extrapolation of the power spectrum within a factor of a few.**

Previous marginal measurement of change in the orbital period, was $(-2.9 \pm 2.1) \times 10^{-6} \text{ yr}^{-1}$ (Clark 2000), and our new value for the orbital period change, $\dot{P}/P = (0.4 \pm 1.8) \times 10^{-6} \text{ yr}^{-1}$, are consistent with zero. These two measurements are consistent with each other in 1σ level.

In most of the X-ray binaries with accretion powered pulsars, the evolution of the orbital period seems to be too slow to be detectable. Yet there are still some such systems in which this evolution was measured and \dot{P}/P were reported. These systems include Cen X-3 with $(-1.8 \pm 0.1) \times 10^{-6} \text{ yr}^{-1}$ (Kelley et al. 1983; Nagase et al. 1992), Her X-1 with $(-1.32 \pm 0.16) \times 10^{-8} \text{ yr}^{-1}$ (Deeter et al. 1991), SMC X-1 with $(-3.36 \pm 0.02) \times 10^{-6} \text{ yr}^{-1}$ (Levine et al. 1993), Cyg X-3 with $(1.17 \pm 0.44) \times 10^{-6} \text{ yr}^{-1}$ (Kitamoto et al. 1995), 4U 1700-37 with $(3.3 \pm 0.6) \times 10^{-6} \text{ yr}^{-1}$ (Rubin et al. 1996), and LMC X-4 with $(-9.8 \pm 0.7) \times 10^{-7} \text{ yr}^{-1}$ (Levine et al. 2000). Change in the orbital period of Cyg X-3 was associated with the mass loss rate from the Wolf-Rayet companion star. For 4U 1700-37, the major cause of orbital period change was also thought to be mass loss from the

companion star. For Her X-1, mass loss and mass transfer from the companion were proposed to be the reasons of the change in the orbital period of the system.

On the other hand, for the high mass X-ray binary systems Cen X-3, LMC X-4 and SMC X-1, the major cause of change in the orbital period is likely to be tidal interactions (Kelley et al. 1983; Levine et al. 2000; Levine et al. 1993). For these three systems, orbital period decreases (i.e. derivative of the orbital period is negative). Our new measurement of orbital period change (\dot{P}/P) gives the value of about -10^{-6} yr^{-1} which is similar to the observed values of SMC X-1 and Cen X-3. Further observations can give further information about the orbital period change of this source.

Acknowledgments

We thank anonymous referee for useful suggestions and comments.

References

- Becker R.H., Swank J.H., Bold E.A., Holt S.S., Pravdo S.H., Saba J.R., Serlemitsos P.J., 1977, *ApJ. Lett.*, 216, L11
- Clark, G.W. 2000, *ApJL*, 542, 133
- Corbet, R.H.D., Woo, J.W., Nagase, F. 1993, *A& A*, 276, 52
- Deeter, J.E., Boynton, P.E., Pravdo, S.H. 1981, *ApJ*, 247, 1003
- Deeter, J.E., Boynton, P.E. 1985, in *Proc. Inuyama Workshop on Timing Studies of X-ray Sources*, ed. S. Hayakawa& F.Nagase (Nagoya: Nagoya Univ.), 29
- Deeter, J.E., Boynton, P.E., Miyamoto, S. et al. 1991, *ApJ*, 383, 324
- Giacconi R., Murray S., Gursky H., Kellog E., Schreier E., Matilsky T., Koch D., Tananbaum H., 1974, *ApJS*, 27,37
- Jahoda, K., Swank, J.H., Giles, A.B., Stark, M.J., Strohmayer, T., Zhang, W., Morgan, E.H., 1996, *Proc. SPIE*, 2808, 59
- Kelley, R.L, Rappaport, G., Clark, G.W., Petro, L.D. 1983, *ApJ*, 268, 790
- Kitamoto, S., Hirano, A., Kawashima, K. et al. 1995, *PASJ*, 47, 233
- Levine, A., Rappaport, S., Deeter, J.E. et al. 1993, *ApJ*, 410, 328
- Levine, A.M., Rappaport, S.A., Zojcheski, G., 2000, *ApJ*, 541, 194
- Makishima K., Koyama K., Hayakawa S., Nagase F., 1987, *ApJ.*, 314, 619
- Nagase, F., Corbet, R.H.D., Day, C.S.R., et al. 1992, *ApJ*, 396, 147
- Parkes, G.E., Murdin, P.G., Mason, K.O. 1978, *MNRAS*, 184, 73
- Rubin, B.C., Finger, M.H., Harmon, B.A. et al. 1996, *ApJ*, 459, 259
- Rubin, B.C., Finger, M.H., Scott, D.M. et al. 1997, *ApJ*, 488, 413